

## Model-Based Fiducial Points Extraction for Baseline Wandered Electrocardiograms

Omid Sayadi\*, *Student Member, IEEE*, and  
 Mohammad B. Shamsollahi, *Member, IEEE*

**Abstract**—A fast algorithm based on the nonlinear dynamical model for the electrocardiogram (ECG) is presented for the precise extraction of the characteristic points of these signals with baseline drift. Using the adaptive bionic wavelet transform, the baseline wander is removed efficiently. In fact by the means of the bionic wavelet transform, the resolution in the time-frequency domain can be adaptively adjusted not only by the signal frequency but also by the signal instantaneous amplitude and its first-order differential, which results in a better baseline wander cancellation. At the next step the parameters of the model are chosen to have the least square error with the original ECG. Determining the precise position of the waveforms of an ECG signal with baseline wander is complicated due to the varying amplitudes of its waveforms, the ambiguous and changing form of the complex and the unknown drift. A model-based approach handles these complications, therefore a method based on this concept has been developed and the fiducial points are accurately detected using the center and spread parameters of Gaussian-functions of the model. Simulation results show that the proposed method has an average sensitivity of 99.58%, average detection accuracy of 99.64%, and specificity of 100%.

**Index Terms**—Baseline wander, bionic wavelet transf, electrocardiogram (ECG), ECG dynamical model, fiducial points.

### I. INTRODUCTION

THE NEW generation of medical treatment has been supported by computerized processes. Signals recorded from the human body provide valuable information about the activities of its organs. Their characteristic shape, or temporal and spectral properties, can be correlated with a normal or pathological function. In response to dynamical changes in the behavior of those organs, the signals may exhibit time-varying as well as nonstationary responses. In fact, those signals are always contaminated by drift and interference caused by several bioelectric phenomena, or by various types of noise, like intrinsic noise from the recorder, noise from electrode-skin contact, and any low-frequency interferences.

The focus of this paper is to detect all of the fiducial points related to the five main waveforms in an electrocardiogram (ECG) with baseline wander. Fiducial points in an ECG signal are the onset and offset of P and T waveforms, and the locations of Q, R, and S. Efforts have aimed to cope with the problem of characteristic (fiducial) points extraction in an ECG. Since baseline drifts not only include low-pass interferences but also additive or multiplicative perturbations, linear phase highpass filters would not overcome the problem. In addition, a highpass filter distorts the low frequency components of an ECG. Hence, various algorithms have been proposed for the extraction of the fiducial points of an ECG, and especially the QRS complex [1]. Among them, the

wavelet transform (WT) has the most important role [2], mainly because it provides important information about the mathematical morphology of signals having multiresolution characteristics such as ECG signals. In a recent study, Krimi *et al.* used the wavelet transform modulus maxima to detect the T-waves of the ECG [3]. Wavelet transforms have also been used for the QRS detection [4] and ectopic beat detection [5]. When an ECG is contaminated with a source producing baseline drifts, however, the same methods would not overcome the problem.

Recently and based on the bionic wavelet transform (BWT), we have introduced methods and their applications to noise and baseline wander suppression in ECG [6]–[8] which is exclusively capable of removing all kinds of drifts including effects of DC components and low frequency interferences. On the other hand, research has been conducted towards the generation of synthetic ECG cardiac signals to facilitate the testing of signal processing algorithms in the recent years. Specifically, in [9] and [10] a dynamic model has been developed, which reproduces the morphology of the PQRST complex and their relationship to the beat-to-beat (RR-interval) timing in a single nonlinear dynamic model. Considering the simplicity and flexibility of this model it is reasonable to assume that it can be easily adapted to a broad class of ECGs. The proposed innovative approach includes the following two steps. 1) Using the BWT a baseline corrected version of the initial ECG signal is achieved. 2) The model is fitted to this ECG which tends to describe the signal with a sum of Gaussians. The fiducial points are determined via the parameters of these Gaussians.

The paper is organized as follows. Section II summarizes the dynamical model of an ECG signal. Section III describes the innovative method used for the extraction of fiducial points. Simulation results are provided in Section IV. Finally, summary and conclusions are provided in Section V.

### II. ECG DYNAMICAL MODEL

The model generates a trajectory in a 3-D state-space with coordinates  $(x, y, z)$ . In essence, each feature of the ECG is described by a Gaussian with three parameters; the amplitude, width and phase. The dynamical equations of motion are given by a set of ordinary differential equations as follows:

$$\begin{aligned} \dot{x} &= \alpha x - \omega y \\ \dot{y} &= \alpha y + \omega x \\ \dot{z} &= - \sum_{i \in \{P, Q, R, S, T\}} a_i \Delta \theta_i \exp\left(-\frac{\Delta \theta_i^2}{2b_i^2}\right) - (z - z_0) \end{aligned} \quad (1)$$

where  $\alpha = 1 - \sqrt{x^2 + y^2}$ ,  $\Delta \theta_i = (\theta - \theta_i) \bmod 2\pi$ ,  $\theta = \text{atan2}(y, x)$ ,  $\omega$  is the angular velocity of the trajectory as it moves around the limit cycle, and  $a_i, b_i$  are the amplitude and spread of Gaussian functions, respectively [9]. In this model, the baseline wander of the ECG is modeled with the parameter  $z_0$ , which is a small sinusoidal component coupled with the respiratory frequency. Numerical integration of the last equation using an appropriate set of parameters leads to the familiar ECG waveform,  $z$ . It can be observed that the model generates the sum of five Gaussian functions, corresponding to PQRST, to be a one cycle of the ECG signal. Fig. 1 shows a typical ECG signal and the five Gaussian functions that are to be added to make the original ECG.

### III. METHOD

In order to determine the precise locations of the fiducial points of an ECG waveform with baseline wander, first it is necessary to remove the drift and next to fit the model to the ECG and then to use the fit parameters to describe the onset and offset of the PQRST waves.

Manuscript received October 9, 2006; revised March 30, 2007. This work was supported in part by the Iran Telecommunications Research Center (ITRC) under Grant T/500/15023. Asterisk indicates corresponding author.

\*O. Sayadi is with the Biomedical Signal and Image Processing Laboratory (BiSIPL), Electrical Engineering Department, Sharif University of Technology, Azadi Ave., P.O. Box 11365–9363, Tehran, Iran (e-mail: osayadi@ee.sharif.edu)

M. B. Shamsollahi is with the Biomedical Signal and Image Processing Laboratory (BiSIPL), Electrical Engineering Department, Sharif University of Technology, Tehran, Iran (e-mail: osayadi@ee.sharif.edu)

Digital Object Identifier 10.1109/TBME.2007.899302

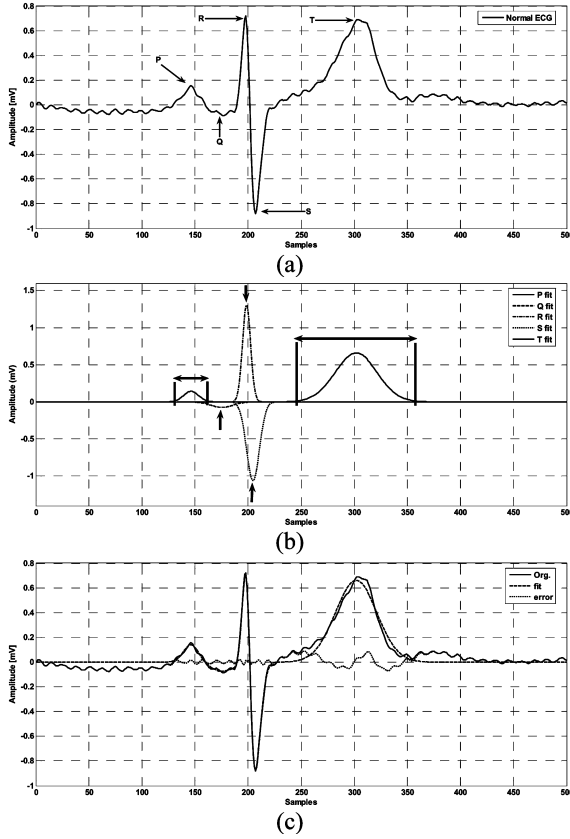


Fig. 1. (a) Real normal ECG waveform. (b) Five Gaussian functions of the model with arrows indicating the fiducial points. (c) Original signal and the sum of five Gaussians.

### A. Baseline Correction With BWT

Previously, Yao and Zhang introduced a novel wavelet transform, called the bionic wavelet transform, which is defined by the following equation [11]:

$$\begin{aligned} BWT_x(\tau, a) &= \int x(t)h_T^* \left( \frac{t-\tau}{a} \right) dt \\ &= \frac{1}{T\sqrt{a}} \int x(t)\tilde{h}^* \left( \frac{t-\tau}{aT} \right) \\ &\quad \times \exp \left( -j2\pi f_0 \left( \frac{t-\tau}{a} \right) \right) dt. \end{aligned} \quad (2)$$

In the above equation,  $h_T(t)$  is the BWT mother function and is considered to have the following form:

$$h_T(t) = \frac{1}{T\sqrt{a}} \tilde{h} \left( \frac{t}{T} \right) \exp(j2\pi f_0 t). \quad (3)$$

As can be seen, in contrast to the wavelet transform, both the amplitude and the time-spread of BWT mother function depend on the  $T$  value. For evaluating the  $T$  parameter, they adopted a general nonlinear form based on a previously introduced auditory model [12]. This results in the following formula for a function, namely the T-function:

$$\begin{aligned} T(\tau + \Delta\tau) &= \left( 1 - \tilde{G}_1 \frac{BWT_s}{BWT_s + |BWT_x(\tau, a)|} \right)^{-1} \\ &\quad \times \left( \frac{1 + \tilde{G}_2 |\partial BWT_x(\tau, a)|}{\partial t} \right)^{-1} \end{aligned} \quad (4)$$

where  $\tilde{G}_1$ ,  $\tilde{G}_2$  and  $BWT_s$  are constants, and  $BWT_x(\tau, a; h)$  is the BWT coefficient at time  $\tau$  and scale  $a$  and  $\Delta\tau$  is the calculation step. They also showed that BWT coefficients can be easily calculated based on the corresponding wavelet transform coefficients.

Recently, we have shown that BWT can be efficient in baseline wander correction if we choose the initial center frequency of the mother function,  $f_0$ , to be 400 Hz [8], and relate it to the center frequency of the  $m$ -th scale,  $f_m$ , using a constant parameter,  $q$ , as follows [11]:

$$f_m = \frac{f_0}{q^m}, \quad q > 1. \quad (5)$$

The implementation of the algorithm is much the same as WT. First the signal is decomposed into different subbands using the BWT, and then the scales corresponding to the baseline drift are simply thresholded. Finally the baseline corrected version of the signal is obtained through the inverse BWT.

### B. Fitting the Model to the Baseline Corrected ECG

For the purpose of fitting the nonlinear dynamical model to the baseline corrected ECG signal, one should solve the following optimization problem:

$$\min_{a_i, b_i, \theta_i} E \{ \|s(t) - z(t)\|_2^2 \} \quad (6)$$

where  $s$  is the ECG signal and  $z$  is described with the following equation [13]:

$$z(a_i, b_i, \theta_i) = \sum_i a_i b_i^2 \exp \left( \frac{-\Delta\theta_i^2}{2b_i^2} \right). \quad (7)$$

A fast implementation of the above problem would be possible with an approximation of the locations of the fiducial points. To approximate the fiducial points, a scheme based on the slope changes of the ECG signal [14] is implemented as described below.

First a slope signal is constructed using the first or the second derivative of the ECG signal [14], or equivalently one can use the slope signal defined as [15]

$$Slope(n) = -2s(n-2) - s(n-1) + s(n+1) + 2s(n+2). \quad (8)$$

The above slope signal is quasi-periodic, reflects changes in the behavior of an ECG, and can be used as an R-detector. For the onset of P and T waves the slope signal tends to be positive and it remains positive until it reaches its peak. As the wave falls, the slope tends to be negative and it remains negative till the wave ends. So it is possible to have an approximation of the onset and offset of the PQRST waveforms, but unfortunately the slope signal itself is not a smooth signal and misleads the thresholds used for point estimation. To solve this problem a threshold is selected so as to preserve  $\alpha\%$  of the signal energy, and a thresholded version of the slope signal is then obtained. After this using a logic comparison, a three level thresholded slope gradient signal (that we call the saturated signal) is achieved which is a more reliable signal to perform thresholding properly. Now the approximated locations of the fiducial points can be determined using the succession of 1, 0, and -1. Fig. 2 shows the steps of the algorithm for an ECG signal chosen from the MIT-BIH arrhythmia database [16]. As can be seen the estimates are appropriate as an initial condition.

### C. Precise Fiducial Points Extraction

As stated before, to determine the exact locations of the fiducial points, i.e., the onset and offset of P and T waves, and the locations of

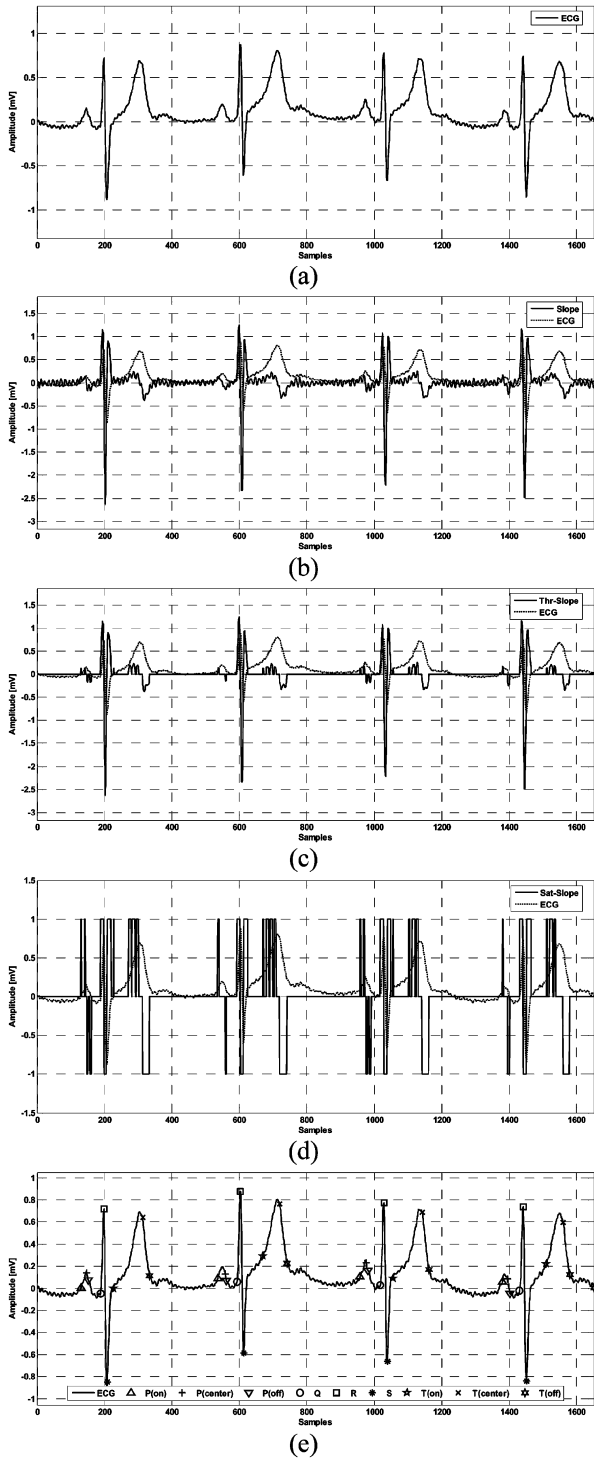


Fig. 2. (a) ECG signal. (b) Slope signal. (c) Thresholded slope signal with  $\alpha = 98\%$ . (d) Saturated slope signal. (e) Fiducial points estimates.

Q, R and S peaks, we use the Gaussian functions of the model which have been fitted to the available ECG signal. To determine the onset and offset of P and T waves, we have used the approximately 99% confidence bound considering the spread parameters,  $b_i$ 's, for the termination of the two Gaussian functions representing these waves. In other words, when any of the two Gaussian functions representing P and T waves in the fitted ECG extends to three times its spread (equal to 99% confidence bound) it is considered as the onset point. The same is true for the offset point. Similarly to detect the QRS peaks, we have used

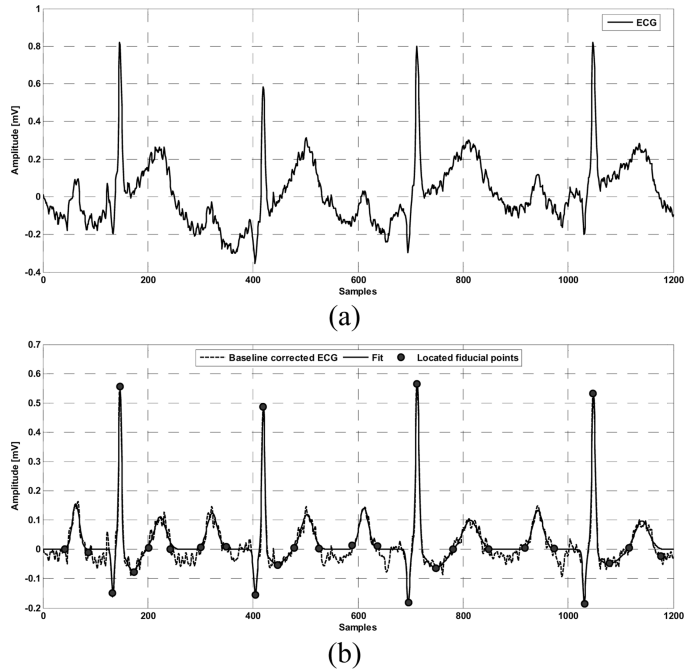


Fig. 3. (a) MIT-BIH ECG No. 228 (analyzed portion: 0.04'': 3.37''). (b) Baseline corrected ECG, and the fitted signal. The precise fiducial points are indicated by ellipses.

the remaining three Gaussians center locations to extract these peaks. To clarify this, refer to Fig. 1(b) which declares the above description. The confidence bounds are indicated with double headed arrows.

#### IV. SIMULATION RESULTS

The proposed method was tested on the MIT-BIH arrhythmia database [16]. For the BWT implementation we have used the following parameters:  $\hat{G}_1 = 0.87$ ,  $\hat{G}_2 = 45$ ,  $BWT_s = 0.8$ , as was stated in [11]. In addition for thresholding, is set to 98%. The performance of the system was verified with manual detection results. The manual detection was used to provide a known reference for the exploration, so these ECG's were first annotated completely by an experienced cardiologist. Furthermore we have used the following parameters to evaluate our method: number of true positive detections ( $TP$ ), number of false positive detections ( $FP$ ), number of true negative detections ( $TN$ ), and number of false negative detections ( $FN$ ). On the basis of this terminology, we can calculate sensitivity ( $Sn$ ) and specificity ( $Sp$ ) criteria, defined as

$$Sp = \frac{TN}{TN + FP}$$

$$Sn = \frac{TP}{TP + FN} \quad (9)$$

Also the accuracy ( $Ac$ ) detection, which is defined as the ratio of number of true detected points to the number of all points, has been calculated for the test signals. Figs. 3 and 4 show the typical results of the algorithm for two different ECG signals. Fig. 3 includes the precise fiducial points specified on the baseline corrected ECG signal while Fig. 4 includes the fiducial points on the original ECG. In fact by determining the locations of the fiducial points on the baseline corrected signal, their locations on the initial ECG can easily be found by correspondence.

For evaluation, we have considered the four types of ECG signals with baseline wander: Normal ECG (ex. ECG No. 222), ECG having low amplitude P and T waves (ex. ECG No. 104), ECG contaminated

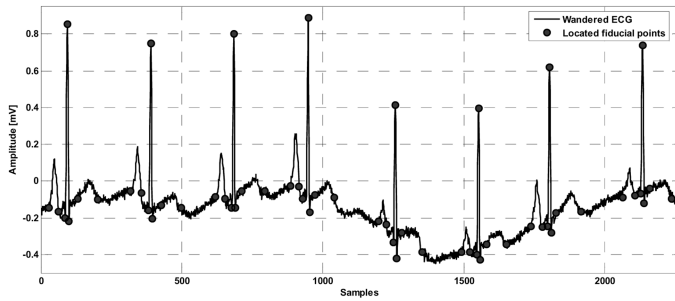


Fig. 4. MIT-BIH ECG No. 222 (analyzed portion: 03.90'': 10.08''), with the precise fiducial points indicated by ellipses on the same signal.

TABLE I  
MODEL-BASED ECG FIDUCIAL POINTS EXTRACTION PERFORMANCE ON THE MIT-BIH ARRHYTHMIA DATABASE

Rec. No.	Length (sec)	TP	FP	FN	Sn (%)	Sp(%)	Ac(%)
222	216	2112	0	2	99.90	100	100
104	222	1848	4	6	99.68	100	99.95
203	242	2420	9	22	99.10	100	98.95
228	388	1697	6	6	99.65	100	99.65
<b>AVERAGE:</b>					<b>99.58</b>	<b>100</b>	<b>99.64</b>

TABLE II  
COMPARING THE SENSITIVITY (Sn %) OF THE TECHNIQUES USED TO DETECT ECG FIDUCIAL POINTS

Selected Approach	Algorithm	Rec. 222	Rec. 104	Rec. 203	Rec. 228
Beat detection	FB [17]	99.81%	99.57%	97.54%	99.65%
	Our method	99.93%	99.73%	99.20%	99.65%
T-wave detection	WTMM [3]	99%	93%	96%	86%
	Our method	99.94%	99.81%	99.09%	99.41%

with noise (ex. ECG No. 203), and ECG with ambiguous waves (ex. ECG No. 228). The records start at 00:00 and have different lengths. Their approximate lengths and evaluation results are provided in Table I. It is worth noting that as we have restricted the model to include only the PQRST waves (i.e., there are only five Gaussian functions) no true negative detections would occur, and consequently the specificity would be 100%.

In order to investigate the validity of results, we have compared our algorithm to two approaches of points extraction, i.e., beat detection (QRS-based) and T-wave detection. The best previously stated results have been considered for both cases. Hence, for the beat detection we have chosen the filter bank (FB) method [17], and for the T-wave extraction, a recently proposed method based on the adjusted WT modulus maxima (WTMM) [3], is considered. The results are provided Table II.

Another point of interest is to investigate the ability of the proposed model-based algorithm for abnormal ECGs such as in bundle branch block or atrial fibrillation, where some of the fiducial points are actually missing or there have waveform repetitions. To overcome this problem we have made modifications to the model which assumes more than five waveforms in a single beat. In addition, we find the amplitude of R wave,  $a_R$ , for each beat. Then, an experimental threshold for the amplitude of P and T waves is set which determines if the related wave exists ( $\geq thr \times a_R$ ) or missed ( $< thr \times a_R$ ). Obviously, the threshold depends on the ECG waveform. Based on preliminary studies on the MIT-BIH database with various thresholds, we found that  $thr = 0.07$  is a good choice for ECG lead V1. The results are shown in Fig. 5 for atrial fibrillation.

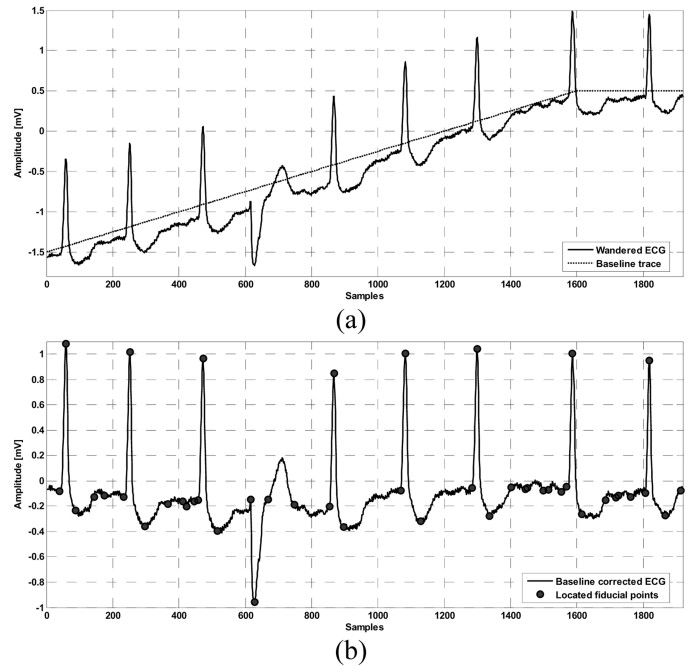


Fig. 5. (a) First 1920 samples of the MIT-BIH ECG No. 210 (Lead V1 with atrial fibrillation), with simulated baseline perturbation, and baseline trace. (b) Baseline corrected ECG. The precise fiducial points are depicted with ellipses.

## V. DISCUSSION AND CONCLUSION

We have presented and validated an ECG fiducial points detection method for baseline wandered ECG signals. A two stage algorithm has been utilized; first, a baseline corrected version of the wandered signal is obtained using the bionic wavelet transform. Second, the ECG dynamic model is fitted to the nonwandered signal using an estimation of the fiducial points. Lastly, the precise fiducial points are determined with respect to the parameters of the Gaussian functions of the model.

In comparison with other proposed methods for point detection, the model-based approach has a superior performance for there is no decision rules based on comparison against thresholds. Approaches based on signal derivatives, digital filters, and neural network classifiers are of this type. But in the model-based method, like filter bank or singularity detection techniques, there is no thresholding. Instead, the points are determined due to the parameters of the Gaussian functions of the model.

In presence of baseline wanders there is a need to use a promising technique for baseline drifts suppression to allow the least mean square error fit. In fact by the means of BWT, the resolution in the time-frequency domain can be adaptively adjusted not only by the signal frequency but also by the signal instantaneous amplitude and its first-order differential. Hence, any kinds of baseline wander would be eliminated efficiently. In order to give an impression about the nature of errors in fiducial point detection using the BWT method, one should be aware of the heart rate and the time periods between different waveforms. These parameters mostly determine the overlap of time-frequency analyzing windows and cause BWT to work less efficiently for ECGs with closely adjacent peaks, which is the result of its intrinsic smoothing property.

Using a nonlinear model enables us to investigate wave morphology variations. To have a good fit, we need an initial estimation for the fiducial points locations. This would probably motivate the algorithm not to be online, and have a computational complexity compared to simpler linear techniques. Typically, the run-time of the algorithm is less than twice that of computationally efficient detectors such as the filter-bank method.

The method has been validated using several ECG records from the MIT-BIH arrhythmia database. None of the more complex cases result in sensitivity less than 98.10% and specificity of 100%, even for ECGs with ambiguous waves. These results show that the developed method provides a reliable and accurate detection of the fiducial points. It outperforms the other algorithms and has an average detection accuracy of 99.64% which is well within the acceptable range. In addition, through simple modifications, it would be robust to PQRST variations, which incorporates several pathological conditions. For highly abnormal ECGs, where some of the fiducial points are missing, an experimental decision rule is used. This gives the opportunity to study very low amplitude complexes, and therefore, it is suited for precise ECG fiducial points detection.

#### ACKNOWLEDGMENT

The authors would like to thank Dr. N. Sadati for his valuable comments and deep knowledge of the problem.

#### REFERENCES

- [1] B. U. Köhler, C. Hennig, and R. Orglmeister, "The principles of software QRS detection," *IEEE Eng. Med. Biol. Mag.*, vol. 21, pp. 42–57, Jan.–Feb. 2002.
- [2] C. Li, C. Zheng, and C. Tai, "Detection of ECG characteristic points using wavelet transforms," *IEEE Trans. Biomed. Eng.*, vol. 42, no. 1, pp. 21–28, Jan. 1995.
- [3] S. Krimi, K. Ouni, and N. Ellouze, "T-Wave detection based on an adjusted wavelet transform modulus maxima," *Int. J. Biomed. Sci.*, vol. 1, pp. 128–132, Feb. 2006.
- [4] S. Kadambe, R. Murray, and G. Boudreaux-Bartels, "Wavelet transform-based QRS complex detector," *IEEE Trans. Biomed. Eng.*, vol. 46, no. 7, pp. 838–848, Jul. 1999.
- [5] D. B. Keenan, "Detection and correction of ectopic beats for HRV analysis applying discrete wavelet transforms," *Int. J. Inf. Technol.*, vol. 2, pp. 54–60, Jan. 2005.
- [6] O. Sayadi and M. B. Shamsollahi, "Multiadaptive bionic wavelet transform: Application to ECG denoising and baseline wandering reduction," in *EURASIP J. Adv. Signal Process.*, 2007, vol. 2007, doi:10.1155/2007/41274.
- [7] O. Sayadi and M. B. Shamsollahi, "ECG denoising with adaptive bionic wavelet transform," in *Proc. EMBS*, 2006, pp. 6597–6600.
- [8] O. Sayadi and M. B. Shamsollahi, "ECG baseline correction with adaptive bionic wavelet transform," in *Proc. ISSPA*, 2007, pp. 1–4.
- [9] P. E. McSharry, G. D. Clifford, L. Tarassenko, and L. A. Smith, "A dynamical model for generating synthetic electrocardiogram signals," *IEEE Trans. Biomed. Eng.*, vol. 50, no. 3, pp. 289–294, Mar. 2003.
- [10] P. E. McSharry and G. D. Clifford, ECGSYN - A Realistic ECG Waveform Generator, Dec. 2003 [Online]. Available: <http://www.physionet.org/physiotools/ecgsyn/>
- [11] J. Yao and Y. T. Zhang, "Bionic wavelet transform: A new time-frequency method based on an auditory model," *IEEE Trans. Biomed. Eng.*, vol. 48, no. 8, pp. 856–863, Aug. 2001.
- [12] J. Yao and Y. T. Zhang, "The application of bionic wavelet transform to speech signal processing in cochlear implants using neural network simulations," *IEEE Trans. Biomed. Eng.*, vol. 49, no. 11, pp. 1299–1309, Nov. 2001.
- [13] G. D. Clifford, A. Shoeb, P. E. McSharry, and B. A. Janz, "Model-based filtering, compression and classification of the ECG," in *Proc. BEM & NFSI*, 2005, pp. 1–4.
- [14] M. A. Haque, M. E. Rahman, C. A. A. Sayeed, and B. M. Z. Uddin, "A fast algorithm in detecting ECG characteristic points," *Proc. ICECE*, pp. 160–163, 2002.
- [15] R. G. Lee, I. C. Choi, C. C. Lai, M. H. Liu, and M. J. Chiu, "A novel QRS detection algorithm applied to the analysis for heart rate variability of patients with sleep apnea," *J. Biomed. Eng., Appl., Basis & Commun.*, vol. 17, pp. 258–262, Oct. 2005.
- [16] The MIT-BIH Arrhythmia Database May 1997 [Online]. Available: <http://physionet.ph.biu.ac.il/physiobank/database/mitdb/>
- [17] V. X. Afonso, W. J. Tompkins, T. Q. Nguyen, and S. Luo, "ECG beat detection using filter banks," *IEEE Trans. Biomed. Eng.*, vol. 46, no. 2, pp. 192–202, Feb. 1999.

## Automated Estimation of the Upper Surface of the Diaphragm in 3-D CT Images

Xiangrong Zhou\*, Hiroaki Ninomiya, Takeshi Hara, Hiroshi Fujita, Ryujiro Yokoyama, Huayue Chen, Takuji Kiryu, and Hiroaki Hoshi

**Abstract**—This communication describes a fully automated method by which the position of the diaphragm surface can be estimated by deforming a thin-plate model to match the bottom surface of the lung in CT images. This method was applied to 338 X-ray CT scans, and its validity was proved by the experimental results.

**Index Terms**—Computer-aided diagnosis (CAD), diaphragm, segmentation, three-dimensional (3-D) image processing, X-ray torso CT images.

### I. BACKGROUND

Modern CT scanners can generate volumetric images with high spatial resolution within 20 to 30 s; these images display the details of the human body. Torso X-ray CT scans are widely used in clinical medicine for lesion detection and surgical operations. However, it is tedious for radiologists to interpret such volumetric images that include over 1000 transverse slices on a monitor or film. Computer-aided diagnosis (CAD) systems that can exhibit the 3-D anatomical structure of the human body and determine the location of suspicious regions are highly expected to reduce the tedium and increase the accuracy of medical image interpretation.

Recognition of the anatomical structures of the human body is the first step in the development of a CAD system. Further, for torso CT images, identification of the diaphragm and the subsequent division of the torso into regions (chest and abdomen) is an important initial step for anatomical structure recognition. Beichel *et al.* proposed a diaphragm surface extraction approach using a semiautomatic process [1]. However, a fully automated process for diaphragm identification and body cavity division is required for the development of a CAD system. In this communication, we propose an automated scheme to locate the upper surface of the diaphragm in noncontrast CT images, and we evaluate its performance by using a large database of torso CT images.

### II. METHODS

The diaphragm is located below the lungs and above the liver. The shape of the diaphragm is not uniform and changes with breathing. Moreover, it is composed of muscles that have a similar density (CT

Manuscript received September 27, 2006; revised March 31, 2007. This research work was a part of the Future-CAD Project under the Grant-in-Aid for Scientific Research on Priority Areas, Japanese Government. *Asterisk indicates corresponding author.*

\*X. Zhou is with the Department of Intelligent Image Information, Division of Regeneration and Advanced Medical Sciences, Graduate School of Medicine, Gifu University, Yanagido 1-1, Gifu 501-1194, Japan (e-mail: [zxr@fjt.info.gifu-u.ac.jp](mailto:zxr@fjt.info.gifu-u.ac.jp)).

H. Ninomiya, T. Hara, and H. Fujita are with the Department of Image Information, Division of Regeneration and Advanced Medical Sciences, Graduate School of Medicine, Gifu University, Gifu 501-1194, Japan.

R. Yokoyama, T. Kiryu, and H. Hoshi are with the Department of Radiology, Gifu University School of Medicine and Gifu University Hospital, Gifu University, Gifu 501-1194, Japan.

H. Chen is with the Department of Anatomy, Graduate School of Medicine, Gifu University, Gifu 501-1194, Japan.

Color versions of one or more of the figures in this paper are available online at <http://ieeexplore.ieee.org>.

Digital Object Identifier 10.1109/TBME.2007.899337